Science of the Total Environment 479–480 (2014) 151–158

Contents lists available at ScienceDirect

Science of the Total Environment

journal homepage: www.elsevier.com/locate/scitotenv

Black carbon aerosol characterization in a remote area of Qinghai–Tibetan Plateau, western China

Qiyuan Wang [a,b], J.P. Schwarz [c,d], Junji Cao [a,e,*], Rushan Gao [c], D.W. Fahey [c,d], Tafeng Hu [a], R.-J. Huang [f,g], Yongming Han [a], Zhenxing Shen [b]

[a] Key Laboratory of Aerosol Science & Technology, SKLLQG, Institute of Earth Environment, Chinese Academy of Sciences, Xi'an 710075, China
[b] Department of Environmental Science and Engineering, Xi'an Jiaotong University, Xi'an 710049, China
[c] National Oceanic and Atmospheric Administration, Earth System Research Laboratory, NOAA, Boulder, CO, USA
[d] Cooperative Institute for Research in Environmental Sciences, University of Colorado, Boulder, CO, USA
[e] Institute of Global Environmental Change, Xi'an Jiaotong University, Xi'an 710049, China
[f] Laboratory of Atmospheric Chemistry, Paul Scherrer Institute, 5232 Villigen PSI, Switzerland
[g] Centre for Climate and Air Pollution Studies, Ryan Institute, National University of Ireland Galway, University Road, Galway, Ireland

HIGHLIGHTS

- Atmosphere over northeast Tibetan Plateau is not pristine, with an average rBC mass concentration of 0.36 μg STP-m^{-3}.
- About 50% of the observed rBC aerosol particles are thickly coated by non-BC materials.
- Non-BC aerosol species affect the Aethalometer measurements at Qinghai Lake.

ARTICLE INFO

Article history:
Received 30 November 2013
Received in revised form 24 January 2014
Accepted 25 January 2014
Available online 19 February 2014

Keywords:
Refractory black carbon
Size distribution
Mixing state
Tibetan Plateau

ABSTRACT

The concentrations, size distributions, and mixing states of refractory black carbon (rBC) aerosols were measured with a ground-based Single Particle Soot Photometer (SP2), and aerosol absorption was measured with an Aethalometer at Qinghai Lake (QHL), a rural area in the Northeastern Tibetan Plateau of China in October 2011. The area was not pristine, with an average rBC mass concentration of 0.36 μg STP-m^{-3} during the two-week campaign period. The rBC concentration peaked at night and reached the minimal in the afternoon. This diurnal cycle of concentration is negatively correlated with the mixed layer depth and ventilation. When air masses from the west of QHL were sampled in late afternoon to early evening, the average rBC concentration of 0.21 μg STP-m^{-3} was observed, representing the rBC level in a larger Tibetan Plateau region because of the highest mixed layer depth. A lognormal primary mode with mass median diameter (MMD) of ~175 nm, and a small secondary lognormal mode with MMD of 470–500 nm of rBC were observed. Relative reduction in the secondary mode during a snow event supports recent work that suggested size dependent removal of rBC by precipitation. About 50% of the observed rBC cores were identified as thickly coated by non-BC material. A comparison of the Aethalometer and SP2 measurements suggests that non-BC species significantly affect the Aethalometer measurements in this region. A scaling factor for the Aethalometer data at a wavelength of 880 nm is therefore calculated based on the measurements, which may be used to correct other Aethalometer datasets collected in this region for a more accurate estimate of the rBC loading. The results present here significantly improve our understanding of the characteristics of rBC aerosol in the less studied Tibetan Plateau region and further highlight the size dependent removal of BC via precipitation.

1. Introduction

Black carbon (BC), a byproduct of incomplete combustion, is the most efficiently light-absorbing aerosol component in the atmosphere. BC plays a major role in climate change (IPCC, 2007) and has been identified as the second largest contributor to anthropogenic radiative forcing (Jacobson, 2001). Due to its non-uniform spatial and temporal distribution, BC can induce significantly higher regional forcing than CO_2 and methane (Chung et al., 2005, 2010). BC's global, direct, anthropogenic radiative forcing is estimated to be ~0.71 W m^{-2} in 2005 (Bond et al., 2013), while regional surface forcing in northern India, for example, can reach as high as 62 W m^{-2} (Tripathi et al., 2005).

The radiative properties of BC, and hence its climate-related impacts, strongly depend on its mixing state. The internal mixture of BC with

* Corresponding author. Tel: +86 29 8832 6488; fax: +86 29 8832 0456.
E-mail address: cao@loess.llqg.ac.cn (J. Cao).

http://dx.doi.org/10.1016/j.scitotenv.2014.01.098

other particulate matter can enhance the absorption of solar radiation by a factor of about 1.5–2.0 compared to externally mixed BC (Bond et al., 2006; Schnaiter et al., 2005). The mixing state of freshly emitted BC depends on combustion conditions. As the emission plume ages, BC becomes internally mixed through a variety of mechanisms including condensation of emitted semi volatile organic compounds and products from photochemical oxidation (Oshima et al., 2009; Petters et al., 2006).

In addition, the impact of BC on the radiation budget may lead to additional consequences, such as global dimming (Wild et al., 2007), decreased crop yields (Chameides et al., 1999), and negative impacts on terrestrial and aquatic ecosystems (Forbes et al., 2006). Further, BC is also associated with adverse impacts on human health (Pope and Dockery, 2006).

Asia has been identified as a region where large amounts of BC are emitted. However, previous studies on BC focused mainly on rural and urban China (e.g., Cao et al., 2007; Han et al., 2008). Here, we concern BC in the Tibetan Plateau (a remote region of China) where studies of BC are very scarce to date and have applied filter-based techniques that measure bulk aerosol absorption rather than specific BC mass concentration (e.g., Cao et al., 2009a, 2010; Engling et al., 2011). Due to the systematic limitations of most of the current filter-based BC measurements (Bond et al., 2013), direct examination of the BC size distribution and mixing state is not feasible.

Here we report measurements of the refractory black carbon (rBC) mass content of individual aerosol particles at the shore of Qinghai Lake in the Tibetan Plateau region detected with a Single Particle Soot Photometer (SP2) instrument. The rBC content measured by the SP2 corresponds closely (Kondo et al., 2011a) to BC as defined in Bond et al. (2013). The SP2 provides rBC mass concentrations, size distributions, and mixing states based on individually detected particles (Schwarz et al., 2006). The high selectivity of the SP2 response to rBC mass ensures that other light-absorbing species do not contribute to the rBC quantification. Further, an Aethalometer, a filter based instrument, was used to measure the total fine-mode aerosol absorption.

Qinghai Lake (QHL), the largest lake in China, is located 3200 m above the sea level in a drainage basin on the Northeast Tibetan Plateau (Fig. 1). Its size and location (i.e. at the junction point of three major climate systems: the East Asian monsoon, the Indian monsoon, and the Westerly) make it very sensitive to climate changes (An et al., 2012). The ecological status of QHL has attracted great attention worldwide (Lister et al., 1991; Jin et al., 2010). The primary objectives of the QHL study were i) to quantify rBC mass concentrations, size distributions, and mixing states in the region at the season of the measurements, and ii) to derive a suitable scaling factor for Aethalometer measurements in this region/season by comparing simultaneous measurements of SP2 and Aethalometer.

2. Methodology

2.1. Research site

Measurements were taken from 16 to 27 October, 2011 from the rooftop (~15 m above ground level) of a sampling tower at the "Bird Island" peninsula (36.98°N, 99.88°E, 3200 m AMSL), which is located at the northwest section of the QHL shore as shown in Fig. 1. There are four counties around QHL (Fig. 1), including Gangcha, Haiyan, Gonhe, and Tianjun, with a total population of ~230,000. Urban areas are located ~180 km to the southeast of QHL. Although it is a remote region, the traffic flow (in particular diesel vehicles) in the QHL basin is significant because of a national highway surrounding the lake. Biofuels including yak and sheep dung, firewood, and crop residues are the main energy sources in the rural areas of Qinghai, and account for ~80% of total household energy, of which ~65% is from burning of and sheep dung (Ping et al., 2011). Trash burning is also customary in the region.

2.2. Instrument description

The operating principles of the SP2 have been described in detail elsewhere (Schwarz et al., 2006; Gao et al., 2007). Briefly, the SP2 measures rBC mass in individual rBC-containing particles using intense,

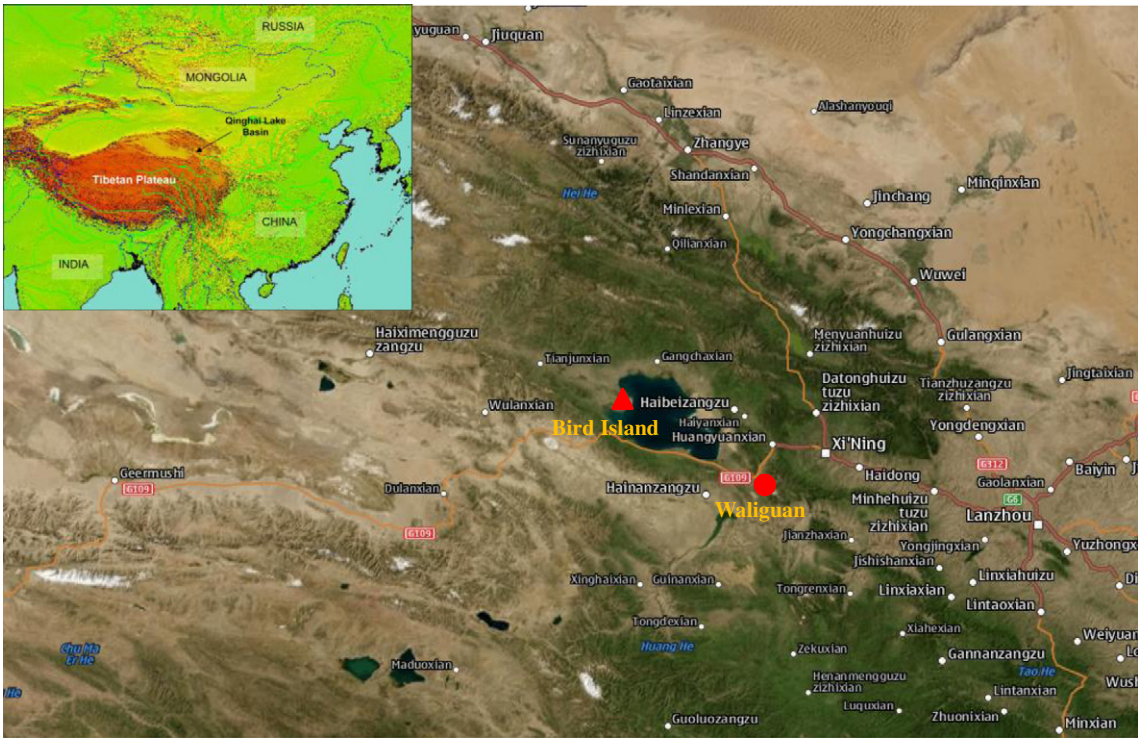

Fig. 1. Map showing the measurement site at Qinghai Lake and the surrounding region.

intracavity laser light at a wavelength of 1064 nm. When a rBC-containing particle passes through the laser beam, the rBC component is heated to its vaporization temperature (~4000 K) and emits incandescent light. The intensity of the incandescence signal is linearly related to the rBC mass and independent of the particle morphology or mixing state over most of the rBC mass ranges observed typically in the accumulation mode (Slowik et al., 2007). Here, the rBC mass in the range of ~0.4–1050 fg, equivalent to 70–1000 nm diameter volume equivalent diameter (VED) assuming 2.0 g cm^{-3} void-free density, was quantified. This range covers >90% of the rBC mass in the accumulation mode. Note that the SP2 only quantifies the mass of the most refractory and light absorbing component of the combustion aerosol, which we generally refer to as black carbon (BC) as in Bond et al. (2013). We use the term "BC-containing particle" to refer to aerosol particles containing this material irrespective of the presence of non-BC materials.

The incandescence signal was calibrated before and after the sampling period using a well-studied standard fullerene soot sample (Lot F12S011, Alpha Aesar, Inc., Ward Hill, Massachusetts). The fullerene soot was size selected by a differential mobility analyzer (DMA) over a range corresponding to rBC of ~0.8–20 fg mass, based on the mass-mobility relationships of this material discussed in Moteki and Kondo (2010). This mass range corresponds to ~90–270 nm VED, over which the calibration was close to purely linear ($r = 0.999$). Monodisperse polystyrene latex spheres (PSL) of different sizes were used to calibrate light-scattering signals measured by the SP2. PSL particles of 269 nm diameter were used daily to monitor SP2 laser intensity to ensure the stability of the SP2 and a sufficient laser power for proper detection of rBC during the entire campaign period (Schwarz et al., 2010).

The total uncertainty in the rBC mass determination was ~25%, estimated from the square root of uncertainties in the rBC mass calibration including possible variability in the SP2 response to ambient rBC mass (~20%, Moteki and Kondo, 2010; Laborde et al., 2012), sample flow (~10%), and estimation of rBC mass beyond of SP2 detection range (~10%). The SP2 sampled air through a cyclone inlet (URG, Chapel Hill, NC), limiting the sizes of ambient particles entering the instrument to <1.0 μm or <2.5 μm diameter depending on setup.

The SP2 data can be interpreted to provide information on the rBC mixing state. The time delay between the peaks in the scattered light signal and the incandescence signal is an indicator of the amount of non-BC material internally mixed with individual rBC masses (here generically referred to as a "coating") (Schwarz et al., 2006; Moteki and Kondo, 2007). This approach is commonly used to distinguish "thinly" and "thickly" coated rBC masses. The delay occurs because coating must be removed from the rBC fraction before the onset of incandescence. Due to saturation of the scattered light detector, the coating state can be determined for rBC core <275 nm VED, which often constitutes a large majority of rBC particle numbers. Note that the method described here does not distinguish thinly coated rBC particles from uncoated rBC particles. Therefore, this method is useful for estimating the relative degrees of internal mixing of rBC-containing particles of different aging and sources, but not capable of specifying the chemical constitute of the coating material on the rBC aerosol. Leading-edge fitting, as in Gao et al. (2007), could not be performed because of flow instability in the aerosol jet of the SP2 (which did not significantly affect rBC mass or peak delay).

An Aethalometer (Model AE-16, Magee Scientific, Berkeley, USA) measured the attenuation of light (880 nm) transmitted through a quartz-fiber filter that collected particles from a continuous ambient air flow (4 L min^{-1}). Light absorption coefficients (σ_{abs}) are derived from the light attenuation measurement (time resolution 5 min) according to Eq. (1):

$$\sigma_{abs} = A/Q \times (\ln(I_1/I_2))/(t_2 - t_1) \quad (1)$$

where I_1 and I_2 are the transmitted light intensities for the aerosol-loaded filter at times t_1 and t_2, respectively; A is the area of the filter in cm^2 that is exposed to the sampling air flow; Q is the amount of sampled air in STP-m^3, which stands for a cubic meter of air at 273.15 K and 1013 hPa. The light absorption coefficients are converted to BC mass concentrations following Eq. (2):

$$BC_{Aeth} = (\sigma_{abs}/\sigma_{ATN}) \quad (2)$$

where σ_{ATN} is a proportionality constant related to the mass absorption cross section (MAC) of aerosol on the filter matrix. The default σ_{ATN} value of 16.6 $m^2\ g^{-1}$ was used. It should be noted that this value is specific for Aethalometer instruments and should not be confused with the real MAC for BC which is on the order of 7.5 $m^2\ g^{-1}$ at 550 nm (Bond and Bergstrom, 2006) for uncoated BC aerosol. Because σ_{abs} measured by the Aethalometer is sensitive to both BC and other particulate matter, BC_{Aeth} derived from the default σ_{ATN} generally does not represent the true atmospheric BC concentrations. Various methods have been developed to correct BC_{Aeth} (Coen et al., 2010 and references therein). However, these correction methods require measurements of total aerosol scattering properties, which are not available in this work. Instead, by comparing with the SP2 data, a scaling factor was calculated to correct the BC_{Aeth} values measured by Aethalometer.

Hourly wind speed (WS) and wind direction (WD) were obtained from the Gangcha National Reference Climatological Station, ~45 km northeast of the sampling site (see Fig. 1). Hourly mixed layer depths (MLDs) during the study period were calculated from the upper-air meteorological data based on the hourly average sounding value archived by the U.S. National Oceanic and Atmospheric Administration (NOAA, http://www.arl.noaa.gov/ready/hysplit4.html).

3. Results and discussion

3.1. rBC mass loading and source

The time series of rBC mass mixing ratios (5 min time resolution) obtained during the campaign are shown in Fig. 2. During the two week sampling period, large daily variability in the concentration was observed, ranging from 0.05 to 1.56 μg STP-m^{-3} with an average (arithmetic mean) value (± standard deviation) of 0.36 ± 0.27 μg STP-m^{-3}. Low concentrations of rBC were observed mainly from late afternoon to early evening, and were generally associated with west/southwest wind (180–290°), whereas enhanced rBC concentrations were observed during the late night and morning when surface winds were from the north/northeast/eastern (0–105°).

Fig. 3 shows the diurnal variation of rBC and meteorological conditions averaged over the entire campaign. The median and mean rBC concentrations have similar diurnal patterns, with minimum values in the late afternoon between 15:00 and 20:00 local standard time (LST) and broad nocturnal maximum values between 23:00 and 02:00 LST. This diurnal cycle can be attributed to the variations in MLDs and WS (see Fig. 3). The nighttime MLDs (see Figs. 2 and 3) were several hundred meters lower than the surrounding mountains (3600–4000 m AMSL), which may lead to the accumulation of locally produced pollutants (within the drainage basin) and thus the high concentrations of rBC at night. The rBC concentrations decreased during the day, which could be attributed to the increased MLDs after sunrise in response to solar heating, the enhanced wind and turbulent dilution. Therefore, the air pollutants in the QHL basin are influenced by regional transport during the day when the MLD is higher than the surrounding maintains, but are isolated at night when the top of the mixing layer is below the basin rim.

Five-day back trajectories (BTs) initiated 150 m above ground level were used to track the potential sources and transport pathways of air pollutants (Fig. 4). The BTs were calculated hourly using the NOAA Air Resource Lab (ARL) HYSPLIT model and gridded meteorological data (Global Data Assimilation System, GDAS1). To minimize the influence from local sources due to the low MLD at night, the data collected during daytime (12:00–19:00 LST) were used when MLDs were higher than

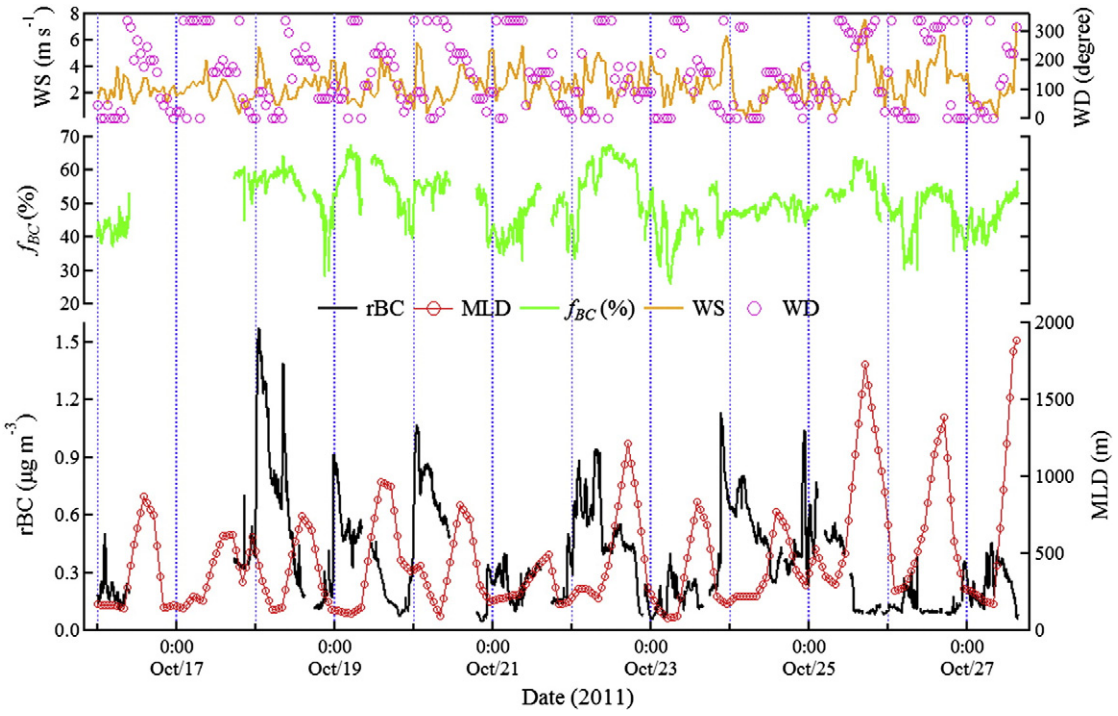

Fig. 2. Time series of 5-min averaged rBC mass concentration and number fraction of thickly coated rBC particles (f_{BC}), as well as the hourly averaged mixed-layer depth (MLD), wind speed (WS) and wind direction (WD) for the entire campaign period.

the surrounding mountains. HYSPLIT was run for those sampling time. As shown in Fig. 4, nearly 70% of air masses were advected from the west where no major rBC sources are found (Lu et al., 2011). During the campaign, the daytime average rBC concentration of 0.21 μg STP-m^{-3} was observed, likely representing the background concentration of rBC in the Tibetan Plateau region. About 20% of air masses stemmed from the east, where large amounts of rBC are emitted from the highly urbanized and industrialized cities Lanzhou and Xining (see Fig. 1),

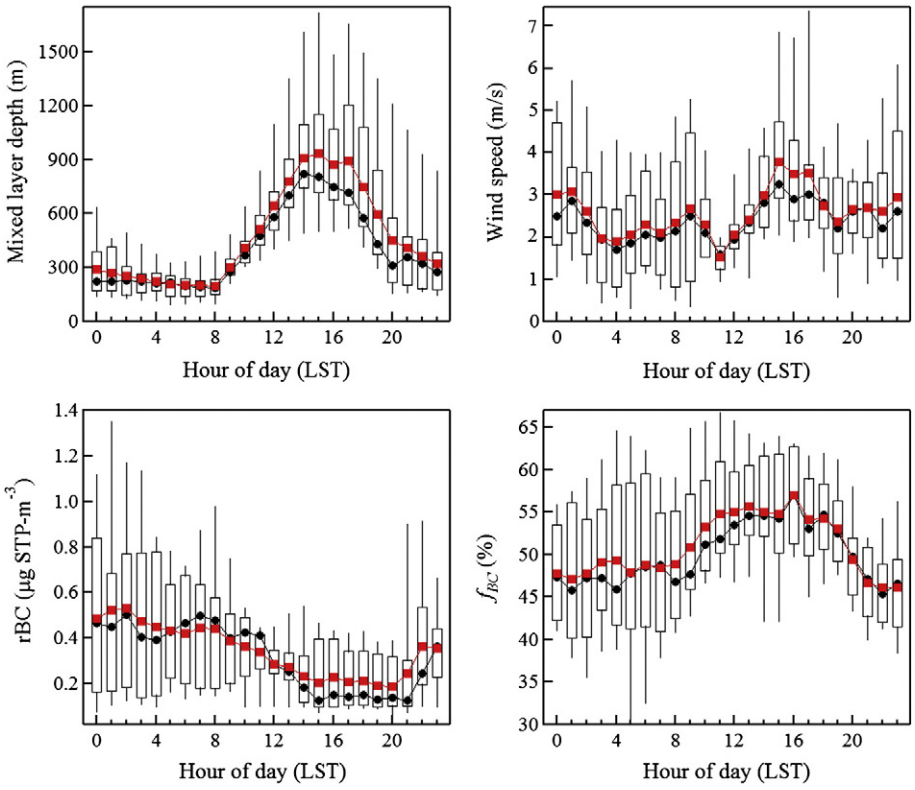

Fig. 3. Diurnal variations of rBC concentration, number fraction of coated rBC particles (f_{BC}), mixed-layer depth, and wind speed. In each box, the upper and lower edges of the box denote the 25% and 75% percentiles, respectively. The black and red lines in the middle of box indicate the median and mean values, with error bars explaining the 10% and 90% percentiles.

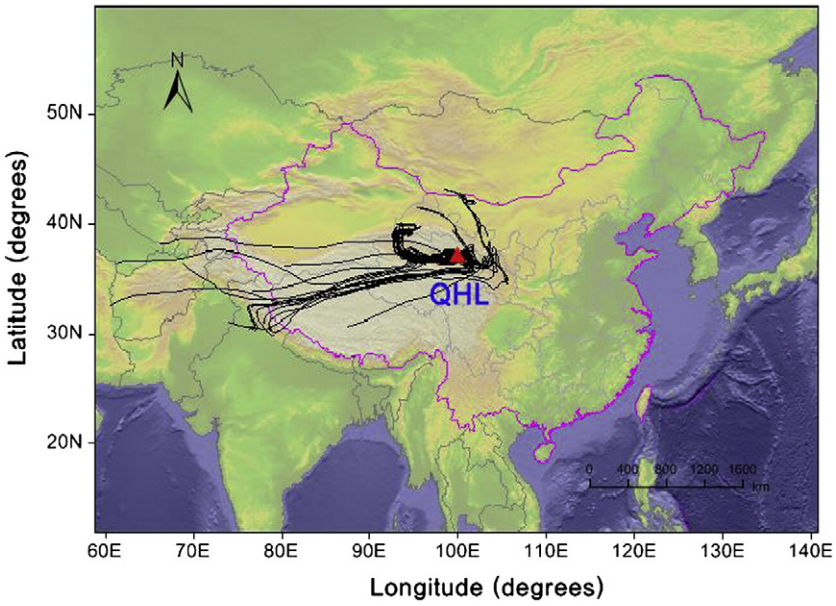

Fig. 4. Five-day backward air mass trajectories reaching at Qinghai Lake (QHL) at 150 m above ground during daytime (12:00–19:00).

consistent with high rBC loadings (>0.30 μg STP-m^{-3}) that were observed in more than 60% of the eastern air masses.

Table 1 shows the mean BC concentrations measured at QHL and other remote rural and high alpine areas. The average rBC concentration at QHL was comparable or lower than BC in southeast Tibet and the central Himalayas (0.34–0.99 μg m^{-3}) (Cao et al., 2010; Dumka et al., 2010; Engling et al., 2011; Qu et al., 2009), where high BC concentrations were mainly influenced by long-range transport and regional anthropogenic emissions. The concentrations measured at QHL were ~2–7 times higher than those reported in Central Tibet (Ming et al., 2010), Southern/Western Himalayas (Babu et al., 2011; Marinoni et al., 2010), and Western China (Cao et al., 2009a; Zhao et al., 2012). Our averaged rBC value was ~34% higher than BC_{Aeth} (measured using an Aethalometer) in Waliguan (Ma et al., 2003), the highest Global Atmospheric Watch (GAW) station, roughly 130 km southeast from the sampling site (see Fig. 1). However, when air masses came from the west of QHL during 12:00–19:00 LST, the average rBC concentration was similar to Waliguan, consistent with regional scale influences affecting both sites equally. The elevated nighttime BC concentrations at QHL can be attributed to the local emissions trapped at night when WLDs are low.

3.2. rBC mass size distribution and mixing state

Fig. 5 shows the mass size distributions of rBC observed at different times of the day (12:00–19:00 LST: Time I and 20:00–11:00 LST: Time II), and during a single snowfall event between 00:00 and 07:00 on 25 October 2011. A two-mode lognormal function fits the data well between 70 and 1000 nm in diameter. A two-mode mass size distribution for BC was previously observed in the Pearl River Delta region of China, and was suggested to be associated with mixed fossil and bio-fuel emissions (Huang et al., 2011). The size distributions between Time I and II have similar primary mode mass median diameters at ~175 nm with a geometric standard deviation, σ, of 2.49 for Time I and 2.51 for Time II, respectively, which is within the range of 150–230 nm reported by previous SP2 studies (Huang et al., 2012, and references therein), assuming the same void-free rBC density of 2 g cm^{-3} for valid comparison. Different emission sources produce rBC size distributions with different mode peaks. McMeeking et al. (2010) found an rBC modal diameter of ~165 nm in the urban plume in Liverpool, Manchester, while the modal diameter in a Texas urban plume was ~170 nm (Schwarz et al., 2008). The rBC peak diameter in a biomass burning plume in Asia was reported to be ~210 nm (Kondo et al., 2011b), similar to a biomass burning plume in Texas (~210 nm) (Schwarz et al., 2008).

The mass median diameter of the secondary mode, which is similar to the one reported by Huang et al. (2011), showed variability within the day, ranging from ~470 nm from Time II when local pollutants were accumulated and aged to ~500 nm from Time I when it was influenced by regional sources. In contrast, measurements made during snow fall reveal that the amplitude of the secondary mode (MMD: ~460 nm) was reduced by one-half with respect to the primary mode (MMD: ~175 nm VED) during this period. The statistical uncertainty of this reduction was small, about 15% of the change. BTs showed that the air mass source region was rather constant before, during, and after the snowfall. Hence this observation suggests that snowfall can remove larger rBC particles more efficiently than smaller rBC particles. This is consistent with the very recent findings of Schwarz et al. (2013) which show the rBC size distributions in snow can be larger than those typically seen in the atmosphere. Note that this is the second study reporting the large secondary mode that is so far observed in China only. We expect that the secondary mode is likely a common feature of BC distributions in regions with biofuel/open fire burning sources.

The number fraction of thickly coated rBC (f_{BC}) is a useful parameter in identifying the relative extent of rBC coating in different ambient samples (Subramanian et al., 2010; McMeeking et al., 2011). Fig. 2 presents the time series of f_{BC} values during the sampling period. The value of f_{BC} ranged from 25 to 68%, with an average of 50 ± 8%. Fig. 3 shows that a clear enhancement of coated rBC number fraction appeared between 12:00 and 19:00 LST, associated with high temperature and low rBC concentrations. This can be explained by the enhanced formation of condensable materials via photochemical oxidation processes in the afternoon. As shown in Fig. 2, the coating fraction is not correlated with rBC concentration ($r = 0.29$), reflecting different sources of the rBC and its associated coatings. The variability in rBC mixing state was observed to be larger during the day than at night, which may be due to the decreased impact of secondary aerosol through photochemical oxidation at night, and more sensitivity to individual local sources.

3.3. Qinghai Lake Aethalometer scaling factor

A correction is needed for Aethalometer measurements to report accurate BC concentrations (Coen et al., 2010). Since the SP2 is capable of

Table 1
The average BC concentration at Qinghai Lake and the remote, rural and high alpine areas.

Location	Type of location	Altitude (m asl)	Period	High BC sources	Method[a]	BC (μg m^{-3})	References
Qinghai Lake, NE Tibet	Remote rural	3200	Oct.2011 (all data) 12:00–19:00 LST	Qinghai Lake basin local pollution Regional influenced by west and northeast of Qinghai Lake	SP2	0.36 0.21	This study
Nam Co, Central Tibet	Remote rural	4730	Jul. 2006–Jan, 2007	Originated from Southern Asia	TOR	0.08	Ming et al., 2010
Mt. Waliguan, NE Tibet	Remote mountain	4000	Oct.–Nov. 1997/Jan. 1998	Influenced by northeastern cities	Aeth.	0.27	Ma et al., 2003
Linzhi, Southeast Tibet	Mountain Glacier	3300	Jan. 2009	Eastern Indian and Bangladesh	Aeth.	0.76	Cao et al., 2010
Tengchong County, SE Tibet	Remote rural	1640	Apr.–May 2004	Influenced by Southeast Asia and local residential activities	Aeth.	0.42	Engling et al., 2011
Zhuzhang, SE Tibetan	Remote rural	3583	Jul. 2004–Mar. 2005	Regional anthropogenic emissions	TOR	0.34	Qu et al., 2009
Manora Peak, Central Himalayas	High-alpine	1958	Nov. 2004–Dec. 2007	Convective boundary layer and increased local emissions	Aeth.	0.99	Dumka et al., 2010
NCO-P, Southern Himalayas	Remote mountain	5079	Mar. 2006–Mar. 2008	Regional circulation and westerly air masses from the Middle East	MAAP	0.16	Marinoni et al., 2010
Hanle, Western Himalayas	Remote mountain	4520	Aug. 2009–Jul. 2010	Advection from West and Southwest Asia	Aeth.	0.08	Babu et al., 2011
Muztagh Ata, Western China	Remote mountain	4500	Dec. 2003–Feb. 2005	Long-range transport from inside China	TOR	0.06	Cao et al., 2009a
Qilian Shan, NW China	Remote mountain	4214	May 2009–Mar. 2011	Influenced by northwest wind	Aeth.	0.05	Zhao et al., 2012

[a] SP2: Single particle soot photometer; TOR: Thermal/optical reflectance; Aeth.; Aethalometer; MAAP: Multi-Angle Absorption Photometer.

measuring rBC accurately, an Aethalometer scaling factor can be obtained by comparing the results from simultaneous SP2 and Aethalometer measurements. Such a scaling factor is only valid when the major composition (e.g. dust fraction, BC fraction, etc.) of the aerosol does not change significantly. A linear correlation between BC_{Aeth} and rBC values is shown in Fig. 6, with a high correlation coefficient of 0.95. The slope, which represents the Aethalometer scaling factor, is 2.49. This scaling factor is consistent with the work of Coen et al. (2010).

To further evaluate the performance of Aethalometer, additional measurements were conducted from 27 June to 3 July, 2012 at an urban site on the rooftop (~10 m above ground level) of the Institute of Earth Environment, Chinese Academy of Sciences (IEECAS; Cao et al., 2009b) in Xi'an, China using the identical SP2 and Aethalometer

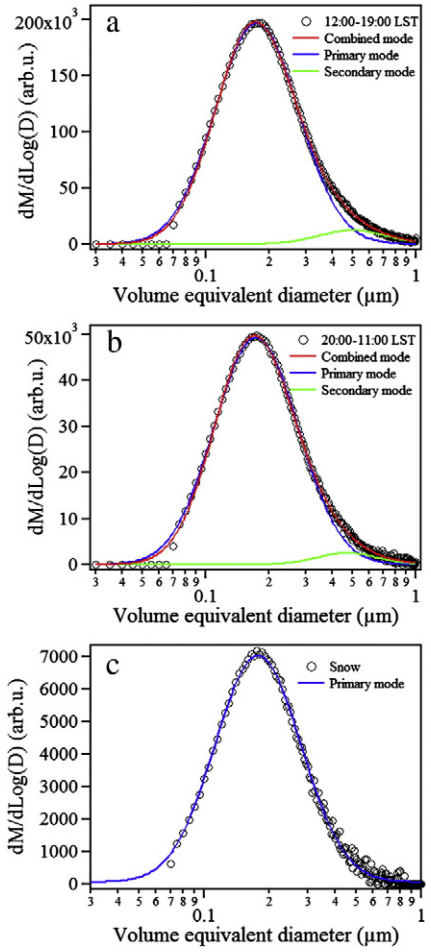

Fig. 5. Size distribution of rBC and the lognormal fitting to the primary, secondary and combined modes at a) 12:00–19:00 and b) 20:00–11:00, c) a single snowfall. "M" and "D" in vertical label represent rBC mass and void free diameter (assuming 2 g cm^{-3} density) respectively.

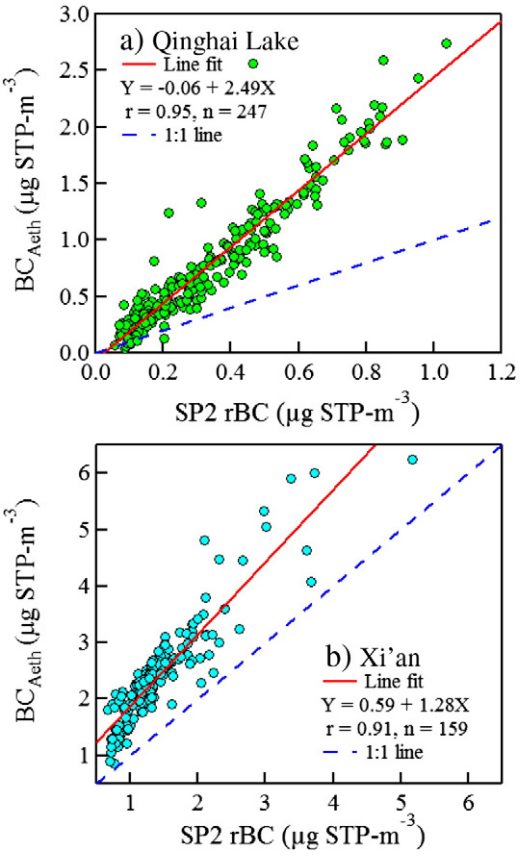

Fig. 6. Correlations between BC concentrations measured by the Aethalometer and rBC concentrations measured by the SP2 from 16 to 27 October, 2011 at Qinghai Lake and from 27 June to 3 July, 2012 in Xi'an. Each data point represents a 50-min average of the concentration.

instruments. Excellent correlation between the two instruments was also observed in Xi'an. However the scaling factor (1.28) is much lower than the value obtained at QHL. This discrepancy may result from the difference in aerosol sources and mixing state of BC. For example, BC at Xi'an site was found to be dominated by fresh vehicular exhausts and coal combustion (Cao et al., 2005, 2009b), which typically represents externally mixed BC. However, at QHL the large emission of BC and organic vapors from open biofuel burning and subsequent aging could lead to enhanced internal mixing of BC with organic carbon (OC). Also increasing OC content may affect the Aethalometer measurement. Lan et al. (2011) also found a relatively low scaling factor of 1.0 in Shenzhen, another urban area of China. The large scaling factor obtained at QHL indicates that non-BC absorbing aerosol species strongly affect the Aethalometer measurements. Therefore, careful examination and correction of the Aethalometer data are still necessary for BC measurements made in the Tibetan Plateau region.

The Aethalometer data did not show changes relative to the SP2 data when the inlet cyclone cutoff diameter was changed between 1.0 and 2.5 μm, suggesting that ambient particles in the size range of 1.0 to 2.5 μm did not affect the Aethalometer measurements. A priori, we would expect that if dust aerosol contributed significantly to the Aethalometer scaling factor, then the change in aerosol size cutoff would, in fact, lead to a shift of the result. Hence, dust aerosol is likely not a major contributor to total aerosol absorption in the QHL boundary layer during the measurement period.

4. Conclusions

An SP2 and an Aethalometer were deployed at Qinghai Lake in the NE Tibetan Plateau from 16 to 27 October 2011 to characterize rBC mass size distribution and mixing state, and to determine the relationship of rBC loading to the Aethalometer-measured aerosol absorption in this region. Based on a two-week sampling period, the average rBC mass concentration (0.36 μg STP-m^{-3}) was not representative of a pristine environment, and was significantly higher than rBC concentrations typically measured in other remote regions. A clear diurnal cycle was observed with rBC concentration reaching a minimum in the late afternoon and peaking at night. This diurnal cycle can be explained by the high mixed layer depth and increased ventilation during the day, and the low mixed layer depth and trapped local emissions (e.g., biofuel burning) at night.

The rBC size distributions show a two-mode lognormal pattern which may represent the features of mixed rBC sources in the QHL region. The modal diameter of the primary mode at ~175 nm, while the secondary modes geometric mean diameter varied within the day, from ~500 nm from 12:00 to 19:00 LST to ~470 nm from 20:00 to 11:00 LST. The secondary mode constitutes generally less than ~10% of the total rBC mass. This mode may be associated with different emission sources and combustion conditions. During a snowfall event, the secondary mode was significantly decreased relative to the primary mode, consistent with very recent findings which show that rBC size in snow can be larger than that typically observed in the ambient atmosphere (Schwarz et al., 2013).

The average number fraction of thickly coated rBC was found to be 50% with higher values in the afternoon, suggesting enhanced formation of organic coating materials produced from photochemical oxidation. The inter-comparison between Aethalometer and SP2 shows that Aethalometer measurements overestimate rBC concentrations at QHL and that careful correction for additional absorption is needed for Aethalometer data obtained at QHL. A scaling factor of 2.49 was derived to correct the Aethalometer measurements at QHL.

Back trajectory analysis indicates that the high-MLD daytime measurements at QHL are likely representatives of the Tibetan Plateau. Together with previous measurements in the Tibet region, our results show that rBC concentrations in the Tibetan Plateau are unexpectedly high (0.21 μg STP-m^{-3}). This unexpected rBC loadings, together with high surface albedo due to the large coverage of snow/ice in this region, can result in significant atmospheric heating. Further study of rBC is therefore necessary to elucidate the sources and atmospheric processing of rBC aerosol and, ultimately, the impact on climate in the Tibetan Plateau.

Acknowledgments

This project is supported by the Natural Science Foundation of China (NSFC 40925009), the Ministry of Science and Technology (2007BAC30B01, 2012BAH31B03) and the Chinese Academy of Sciences (KZCX2-YW-BR-10). JPS, RSG, and DWF were supported by the NOAA Atmospheric Composition and Climate Program and the NOAA Health of the Atmosphere Program. The authors thank the Gangcha weather station for providing the meteorological data.

References

An Z, Colman SM, Zhou W, Li X, Brown ET, Jull AT, et al. Interplay between the Westerlies and Asian monsoon recorded in Lake Qinghai sediments since 32 ka. Sci Rep 2012;2:619. http://dx.doi.org/10.1038/srep00619.

Babu SS, Chaubey JP, Moorthy KK, Gogoi MM, Kompalli SK, Sreekanth V, et al. High altitude (~ 4520 m amsl) measurements of black carbon aerosols over western trans-Himalayas: seasonal heterogeneity and source apportionment. J Geophys Res 2011;116:D24201. http://dx.doi.org/10.1029/2011JD016722.

Bond TC, Bergstrom RW. Light absorption by carbonaceous particles: an investigative review. Aerosol Sci Tech 2006;40:27–67.

Bond TC, Habib G, Bergstrom RW. Limitations in the enhancement of visible light absorption due to mixing state. J Geophys Res 2006;111:D20211. http://dx.doi.org/10.1029/2006JD007315.

Bond TC, Doherty SJ, Fahey DW, Forster PM, Berntsen T, DeAngelo BJ, et al. Bounding the role of black carbon in the climate system: a scientific assessment. J Geophys Res 2013;118:5380–552. http://dx.doi.org/10.1002/jgrd.50171.

Cao JJ, Wu F, Chow JC, Lee SC, Li Y, Chen SW, et al. Characterization and source apportionment of atmospheric organic and elemental carbon during fall and winter of 2003 in Xi'an, China. Atmos Chem Phys 2005;5:3127–37.

Cao JJ, Lee SC, Chow JC, Watson JG, Ho K, Zhang RJ, Jin ZD, Shen ZX, Chen GX, Kang YM. Spatial and seasonal distributions of carbonaceous aerosols over China. J Geophys Res 2007;112:D22S11. http://dx.doi.org/10.1029/2006JD008205, 2007.

Cao JJ, Xu BQ, He JQ, Liu XQ, Han YM, Wang G, et al. Concentrations, seasonal variations, and transport of carbonaceous aerosols at a remote Mountainous region in western China. Atmos Environ 2009a;43:4444–52.

Cao JJ, Zhu CS, Chow JC, Watson JG, Han YM, Wang G, et al. Black carbon relationships with emissions and meteorology in Xi'an, China. Atmos Res 2009b;94:194–202.

Cao JJ, Tie XX, Xu BQ, Zhao ZZ, Zhu CS, Li GH, et al. Measuring and modeling black carbon (BC) contamination in the SE Tibetan Plateau. J Atmos Chem 2010;67:45–60.

Chameides WL, Yu H, Liu S, Bergin M, Zhou X, Mearns L, et al. Case study of the effects of atmospheric aerosols and regional haze on agriculture: an opportunity to enhance crop yields in China through emission controls? Proc Natl Acad Sci U S A 1999;96:13626–33.

Chung CE, Ramanathan V, Kim D, Podgorny I. Global anthropogenic aerosol direct forcing derived from satellite and ground-based observations. J Geophys Res 2005;110:D24207. http://dx.doi.org/10.1029/2005JD006356.

Chung CE, Ramanathan V, Carmichael G, Kulkarni S, Tang Y, Adhikary B, et al. Anthropogenic aerosol radiative forcing in Asia derived from regional models with atmospheric and aerosol data assimilation. Atmos Chem Phys 2010;10:6007–24.

Coen MC, Weingartner E, Apituley A, Ceburnis D, Fierz-Schmidhauser R, Flentje H, et al. Minimizing light absorption measurement artifacts of the Aethalometer: evaluation of five correction algorithms. Atmos Meas Tech 2010;3:457–74.

Dumka U, Moorthy KK, Kumar R, Hegde P, Sagar R, Pant P, et al. Characteristics of aerosol black carbon mass concentration over a high altitude location in the Central Himalayas from multi-year measurements. Atmos Res 2010;96:510–21.

Engling G, Zhang YN, Chan CY, Sang XF, Lin M, Ho KF, et al. Characterization and sources of aerosol particles over the southeastern Tibetan Plateau during the Southeast Asia biomass-burning season. Tellus B 2011;63:117–28.

Forbes MS, Raison RJ, Skjemstad JO. Formation, transformation and transport of black carbon (charcoal) in terrestrial and aquatic ecosystems. Sci Total Environ 2006;370:190–206.

Gao RS, Schwarz JP, Kelly KK, Fahey DW, Watts LA, Thompson TL, et al. A novel method for estimating light-scattering properties of soot aerosols using a modified single-particle soot photometer. Aerosol Sci Tech 2007;41:125–35.

Han YM, Han ZW, Cao JJ, Chow JC, Watson JG, An ZS, et al. Distribution and origin of carbonaceous aerosol over a rural high-mountain lake area, Northern China and its transport significance. Atmos Environ 2008;42:2405–14.

Huang XF, Gao RS, Schwarz JP, He LY, Fahey DW, Watts LA, et al. Black carbon measurements in the Pearl River Delta region of China. J Geophys Res 2011;116:D12. http://dx.doi.org/10.1029/2010JD014933.

Huang XF, Sun TL, Zeng LW, Yu GH, Luan SJ. Black carbon aerosol characterization in a coastal city in South China using a single particle soot photometer. Atmos Environ 2012;51:21–8.

IPCC, Summary for Policymakers, Climate Change. The physical science basis. Contribution of working group I to fourth assessment report of the intergovernmental panel on climate change. Cambridge, New York: Cambridge University Press; 2007.
Jacobson MZ. Strong radiative heating due to the mixing state of black carbon in atmospheric aerosols. Nature 2001;409:695–7.
Jin ZD, You CF, Yu TL, Wang BS. Sources and flux of trace elements in river water collected from the Lake Qinghai catchment, NE Tibetan Plateau. Appl Geochem 2010;25:1536–46.
Kondo Y, Sahu L, Moteki N, Khan F, Takegawa N, Liu X, et al. Consistency and traceability of black carbon measurements made by laser-induced incandescence, thermal–optical transmittance, and filter-based photo-absorption techniques. Aerosol Sci Tech 2011a;45:295–312.
Kondo Y, Matsui H, Moteki N, Sahu L, Takegawa N, Kajino M, Zhao Y, Cubison M, Jimenez J, Vay S, Diskin GS, Anderson B, Wisthaler A, Mikoviny T, Fuelberg HE, Blake DR, Huey G, Weinheimer AJ, Knapp DJ, Brune WH. Emissions of black carbon, organic, and inorganic aerosols from biomass burning in North America and Asia in 2008. J Geophys Res 2011b;116:D08204. http://dx.doi.org/10.1029/2010JD015152.
Laborde M, Mertes P, Zieger P, Dommen J, Baltensperger U, Gysel M. Sensitivity of the single particle soot photometer to different black carbon types. Atmos Meas Tech 2012;5:1031–43.
Lan ZJ, Huang XF, He LY, Hu M, Xue L, Sun TL, et al. Comparison of measurement results of several online carbonaceous aerosol monitoring techniques. Acta Sci Nat Univ Pekin 2011;47:159–65. (in Chinese).
Lister GS, Kelts K, Zao CK, Yu JQ, Niessen F. Lake Qinghai, China: closed-basin like levels and the oxygen isotope record for ostracoda since the latest Pleistocene. Palaeogeogr Palaeoclimatol 1991;84:141–62.
Lu Z, Zhang Q, Streets DG. Sulfur dioxide and primary carbonaceous aerosol emissions in China and India, 1996–2010. Atmos Chem Phys 2011;11:9839–64.
Ma JZ, Tang J, Li SM, Jacobson MZ. Size distributions of ionic aerosols measured at Waliguan Observatory: implication for nitrate gas-to-particle transfer processes in the free troposphere. J Geophys Res 2003;108(D17):4541. http://dx.doi.org/10.1029/2002JD003356.
Marinoni A, Cristofanelli P, Laj P, Duchi R, Calzolari F, Decesari S, et al. Aerosol mass and black carbon concentrations, a two year record at NCO-P (5079 m, Southern Himalayas). Atmos Chem Phys 2010;10:8551–62.
McMeeking GR, Hamburger T, Liu D, Flynn M, Morgan WT, Northway M, et al. Black carbon measurements in the boundary layer over western and northern Europe. Atmos Chem Phys 2010;10:9393–414.
McMeeking GR, Morgan WT, Flynn M, Highwood EJ, Turnbull K, Haywood J, et al. Black carbon aerosol mixing state, organic aerosols and aerosol optical properties over the United Kingdom. Atmos Chem Phys 2011;11:9037–52.
Ming J, Xiao C, Sun J, Kang S, Bonasoni P. Carbonaceous particles in the atmosphere and precipitation of the Nam Co region, central Tibet. J Environ Sci 2010;22:1748–56.
Moteki N, Kondo Y. Effects of mixing state on black carbon measurements by laser-induced incandescence. Aerosol Sci Tech 2007;41:398–417.
Moteki N, Kondo Y. Dependence of laser-induced incandescence on physical properties of black carbon aerosols: measurements and theoretical interpretation. Aerosol Sci Tech 2010;44:663–75.
Oshima N, Koike M, Zhang Y, Kondo Y. Aging of black carbon in outflow from anthropogenic sources using a mixing state resolved model: 2. Aerosol optical properties and cloud condensation nuclei activities. J Geophys Res 2009;114:D18202. http://dx.doi.org/10.1029/2008JD011681.
Petters MD, Prenni AJ, Kreidenweis SM, DeMott PJ, Matsunaga A, Lim YB, et al. Chemical aging and the hydrophobic-to-hydrophilic conversion of carbonaceous aerosol. J Geophys Res 2006;33:L24806. http://dx.doi.org/10.1029/2006GL027249.
Ping X, Jiang Z, Li C. Status and future perspectives of energy consumption and its ecological impacts in the Qinghai–Tibet region. Renew Sustain Energy Rev 2011;15:514–23.
Pope III CA, Dockery DW. Critical review: health effects of fine particulate air pollution: lines that connect. J Air Waste Manage 2006;56:709–42.
Qu WJ, Zhang XY, Arimoto R, Wang YQ, Wang D, Sheng LF, et al. Aerosol background at two remote CAWNET sites in western China. Sci Total Environ 2009;407:3518–29.
Schnaiter M, Linke C, Möhler O, Naumann KH, Saathoff H, Wagner R, et al. Absorption amplification of black carbon internally mixed with secondary organic aerosol. J Geophys Res 2005;110:D19204. http://dx.doi.org/10.1029/2005JD006046.
Schwarz JP, Gao RS, Fahey DW, Thomson DS, Watts LA, Wilson JC, et al. Single-particle measurements of midlatitude black carbon and light-scattering aerosols from the boundary layer to the lower stratosphere. J Geophys Res 2006;111:D16207. http://dx.doi.org/10.1029/2006JD007076.
Schwarz JP, Gao RS, Spackman JR, Watts LA, Thomson DS, Fahey DW, et al. Measurement of the mixing state, mass, and optical size of individual black carbon particles in urban and biomass burning emissions. Geophys Res Lett 2008;35:L13810. http://dx.doi.org/10.1029/2008GL033968.
Schwarz JP, Spackman JR, Gao RS, Perring AE, Cross E, Onasch TB, et al. The detection efficiency of the single particle soot photometer. Atmos Meas Tech 2010;44:612–28.
Schwarz JP, Gao RS, Perring AE, Spackman JR, Fahey DW. Black carbon aerosol size in snow. Sci Rep 2013;3:1356. http://dx.doi.org/10.1038/srep01356.
Slowik JG, Cross ES, Han JH, Davidovits P, Onasch TB, Jayne JT, et al. An inter-comparison of instruments measuring black carbon content of soot particles. Aerosol Sci Tech 2007;41:295–314.
Subramanian R, Kok G, Baumgardner D, Clarke A, Shinozuka Y, Campos T, et al. Black carbon over Mexico: the effect of atmospheric transport on mixing state, mass absorption cross-section, and rBC/CO ratios. Atmos Chem Phys 2010;10:219–37.
Tripathi SN, Dey S, Tare V, Satheesh SK. Aerosol black carbon radiative forcing at an industrial city in northern India. Geophys Res Lett 2005;32:L08802. http://dx.doi.org/10.1029/2005GL022515.
Wild M, Ohmura A, Makowski K. Impact of global dimming and brightening on global warming. Geophys Res Lett 2007;34:L04702. http://dx.doi.org/10.1029/2006GL028031.
Zhao S, Ming J, Xiao C, Sun W, Qin X. A preliminary study on measurements of black carbon in the atmosphere of northwest Qilian Shan. J Environ Sci 2012;24:152–9.